

Vibration Analysis of a Vertical Axis Wind Turbine Blade

*K. McLaren*¹, *S. Tullis*² and *S. Ziada*³

¹McMaster University, mclarekw@mcmaster.ca

²McMaster University, stullis@mcmaster.ca

³McMaster University, ziadass@mcmaster.ca

1. Introduction

The motivation for this project arose from an expected vibration source of a small-scale vertical axis wind turbine currently undergoing field-testing. The turbine consists of three 3 metre long vertically aligned blades each fixed to the central shaft by two horizontal arms and separated from one another by an angle of $\theta=120^\circ$. The blade profile is a NACA 0015 with a chord length of 0.4 metres fixed at zero angle of attack to the support arms. The turbine optimally operates at a blade-tip speed ratio (the ratio of the blade rotational velocity to the ambient wind velocity) of 1.6. As the blades turn about the central shaft, they encounter an incident wind that is composed of the ambient wind and the wind due to rotation (Fig. 1). This incident wind results in lift and drag forces on the blades resulting in both a thrust force and a radial force on the turbine arms. Note: In this paper, lift is defined as the force perpendicular to U_{wind} , and drag is defined as the force parallel to U_{wind} .

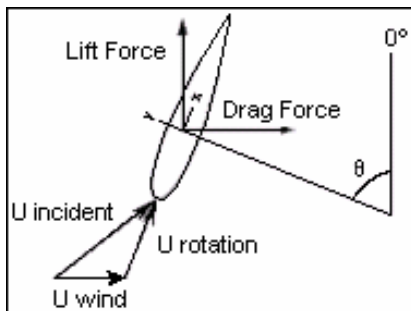


Figure 1: Lift and Drag components on the blade

As the blade completes a full rotation, U_{incident} is expected to vary by $\pm 50\%$ of the mean value while the angle of attack is expected to vary by approx. $\pm 40^\circ$. It is evident that the lift and drag forces on the blade will then also vary in time resulting in cyclic loading on the blades. There is also an expected decrease in flow momentum on the downwind side of the turbine as a result of the passing of the upstream blades.

Initial field tests on the turbine show the existence of significant vibration at three times the frequency of rotation, indicating that aerodynamic loading on the blades may be the cause. In order to better understand the nature of this excitation source, a computational fluid dynamic (CFD) simulation was performed.

2. Numerical Model

The 2D numerical domain was designed to simulate the conditions of the turbine blade flow. A small rotating circular subdomain was contained within a large stationary rectangular domain. A single turbine blade was then located within the rotating subdomain at a radius of 1 metre from the axis of rotation (Fig. 2). The inlet flow condition was fixed at $U_{\text{wind}} = 26.25$ m/s normal to the boundary, with turbulent intensity of 5%. The outlet of the stationary domain was set at an average static pressure of 1 atm. The upper and lower surfaces of the domain were also set with an average static pressure of 1 atm. The surface of the blade was modelled as a smooth no-slip surface. A sliding mesh interface was set at the boundary of the rotating and stationary domains. The diameter of the rotating domain was selected so that the refined mesh surrounding the blade remained within it as it rotates. The rotational velocity of the rotating subdomain was set at 39.38 rad/s giving a blade-tip speed ratio of 1.5. The initial conditions for the domain were the same as the inlet conditions.

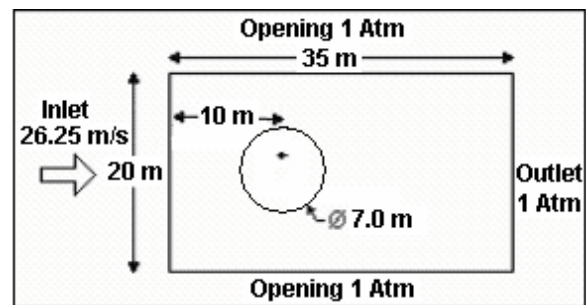


Figure 2: Numerical Domain showing the blade contained within the rotating subdomain

Turbulence was modelled using a blend of the $k-\omega$ model near the blade and the $k-\epsilon$ model away from the blade [1]. A $\gamma-\theta$ intermittency transition model was used to account for the transition from laminar to turbulent flow along the blade [2]. Without the use of a transition model, the separation point location on the blade was poorly predicted. The model was validated against the static wind tunnel results of a NACA 0015 airfoil [3]. As shown in Fig. 3, the numerical results appear to match the experimental data well.

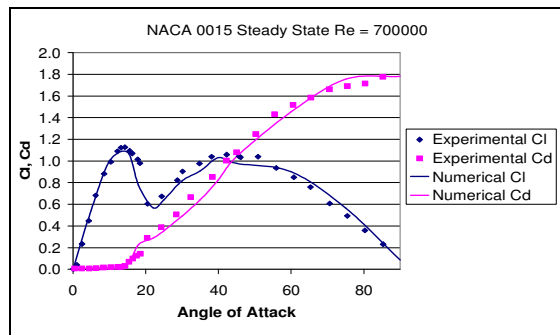


Figure 3: Validation of the model against static wind tunnel test results

3. Results

Three rotations were simulated to ensure initial condition effects were no longer significant and to give time for the wake made by the blade on its upwind pass to be convected across the turbine. Some differences exist in the first rotation due to start-up behaviour, while the solutions for the second and third rotations are nearly identical.

A time step of $1.108 \text{ E-}03 \text{ [s]}$, equivalent to a solution every $\theta=2.5^\circ$ of rotation, was used. This produces small angle of attack changes between time steps and is less than $1/10^{\text{th}}$ the nominal time taken for a "parcel" of air to flow the length of the blade. A Second-Order Backward Euler time advancement scheme was used.

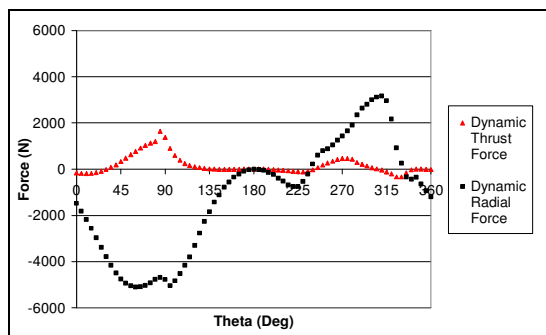


Figure 4: Dynamic thrust and radial force as a function of blade position

Fig. 4 shows the dynamic thrust and radial forces on the blade generated from the data obtained from the third rotation of the transient simulation. It can be seen that on the upwind side of the rotation, $\theta=0^\circ$ to $\theta=180^\circ$, the lift and drag forces on the blade result in a net negative radial force, putting the turbine arms in compression. While on most of the downwind side of the rotation, $\theta=240^\circ$ to $\theta=340^\circ$, the lift and drag forces combine to produce a positive radial force on the blade, putting the arms in tension. However, there is a small region on the downwind side, $\theta=180^\circ$ to $\theta=240^\circ$, where the radial force is negative (arm compression) caused by the blade entering the wake generated on the upwind pass.

Fig. 4 also illustrates that the majority of the thrust force is generated on the upwind pass of the blade between $\theta=40^\circ$ and $\theta=100^\circ$ where the blade is at a moderate relative angles of attack and exposed to high incident wind velocities. Conversely, the region of zero thrust between $\theta=100^\circ$ and $\theta=240^\circ$ exists due to very small relative angles of attack and low incident wind velocities. Once the relative angle of attack and incident flow velocities increase near $\theta=240^\circ$, a small amount of thrust is generated once again. This is followed by a region of the rotation, $\theta=290^\circ$ to $\theta=40^\circ$, where there are small amounts of intermittent negative thrust (i.e. drag).

4. Conclusions

A dynamic CFD model of a vertical axis wind turbine blade has been developed and validated using static experimental data. Dynamic simulations then confirmed the existence of vibration driving forces generated from aerodynamic forces. These results indicate that the majority of the force on the blade is in the radial direction. Furthermore, the dominant frequency of this vibration driving force is equal to the frequency of rotation, resulting in a driving force for all three blades at three times the frequency of rotation, as was expected. Conversely, only a small portion of the force is actually used to drive the turbine and this is achieved in an unsteady oscillating manner. Future simulations with three blades will be performed to study the effect of wakes generated by other blades. These simulations will be validated against dynamic experimental data obtained from the turbine prototype. Once validated, the CFD model will be used to predict aerodynamic and vibration characteristics of future designs.

5. Acknowledgments

The authors gratefully acknowledge the funding support of the Ontario Centres of Excellence and Cleanfield Energy.

References

- [1] F.R. Menter, "Two-equation eddy-viscosity turbulence models for engineering applications." *AIAA Journal*, 32, 1598-1605 (1994).
- [2] F.R. Menter, R.B. Langtry, S.R. Likki, Y.B. Suzen, P.G. Huang, & S. Völker, "A Correlation - Based Transition Model Using Local Variables - Part I: Model Formulation." *Journal of Turbomachinery*, 128, 413-422 (2006).
- [3] Sheldahl, R.E. and Klimas P.C., Aerodynamic Characteristics of Seven Symmetrical Airfoil Sections through 180-Degree Angle of Attack for Use in Aerodynamic Analysis of Vertical Axis Wind Turbines. Sandia National Laboratories Unlimited_Release, 1981.